A Multiscale Observational Case Study of the Development of an Isolated High Plains Tornadic Supercell

MACE L. BENTLEY

Meteorology Program, Northern Illinois University, DeKalb, Illinois

MICHAEL BUBAN

Department of Meteorology, The University of Oklahoma, Norman, Oklahoma

STONIE COOPER

Planetary Data Incorporated, Bennet, Nebraska

9 October 2001 and 24 July 2002

ABSTRACT

On 21 May 1995, a strong tornado developed with an isolated supercell in southwestern Nebraska. Large-scale conditions were not supportive of a tornadic thunderstorm outbreak; however, evidence suggests significant mesoscale enhancements produced a local environment favorable for strong tornado formation. This case study illustrates the importance of ''situation awareness'' and illustrates how mesoscale enhancements must be anticipated by forecasters in order to properly assess rapidly changing atmospheric conditions.

1. Introduction

On 21 May 1995, a thunderstorm in southwestern Nebraska produced a strong (F2) tornado that moved through Perkins County. The tornado developed at 2233 UTC just to the northeast of Madrid, Nebraska, and moved southeast at approximately 7 m s^{-1} (NCDC 1995; Fig. 1). The major structural damage caused by the tornado was within the first 1.6 km of the 8.1-km pathlength (Fig. 1a). A barn, six pivot irrigation systems, and a dozen light poles were destroyed (NCDC 1995). Additionally, a grain bin filled with wooden furniture was demolished, with pieces of furniture found near Highway 23, 4.8 km away. Midway along the damage path, the tornado was nearly 0.8 km wide, as estimated by photographs and damage surveys. However, since the storm was moving over open farmland, tornado intensity could not be estimated because of a lack of structural damage. At 2248 UTC the tornado lifted, and within several minutes, a second tornado (F0) developed west of Elsie, Nebraska, and lasted an additional 10 min.

Observational studies of tornadic thunderstorms and their associated environments have been numerous over the past several decades (Miller 1972; Purdom 1976; Maddox et al. 1980; among others). A consistent finding through many of these investigations has been the proximity of thermal boundaries near the region of tornadogenesis. The alteration of the mesoscale wind and thermodynamic fields by boundaries has been shown to produce a more favorable environment for the production of tornadoes (Markowski et al. 1998; Rasmussen et al. 2000). Evidence suggests that horizontal vorticity generated at boundaries is an important source of low-level rotation in mesocyclones via tilting and stretching (Markowski et al. 1998). Additionally, the preexisting vertical vorticity along boundaries may also be utilized in intensifying the mesocyclone (Maddox et al. 1980).

Several boundaries were present in southwest Nebraska during the late afternoon of 21 May. These boundaries, detectable by surface observations, radar, and high-resolution satellite imagery, appeared to play an important role in the development of this strong tornado in southwestern Nebraska.

2. Data

Surface data used in this study were obtained from the National Weather Service (NWS) Automated Sur-

Corresponding author address: Dr. Mace L. Bentley, Dept. of Geography, Northern Illinois University, Davis Hall, Rm. 115, DeKalb, IL 60115-2895.
E-mail: bentley@geog.niu.edu

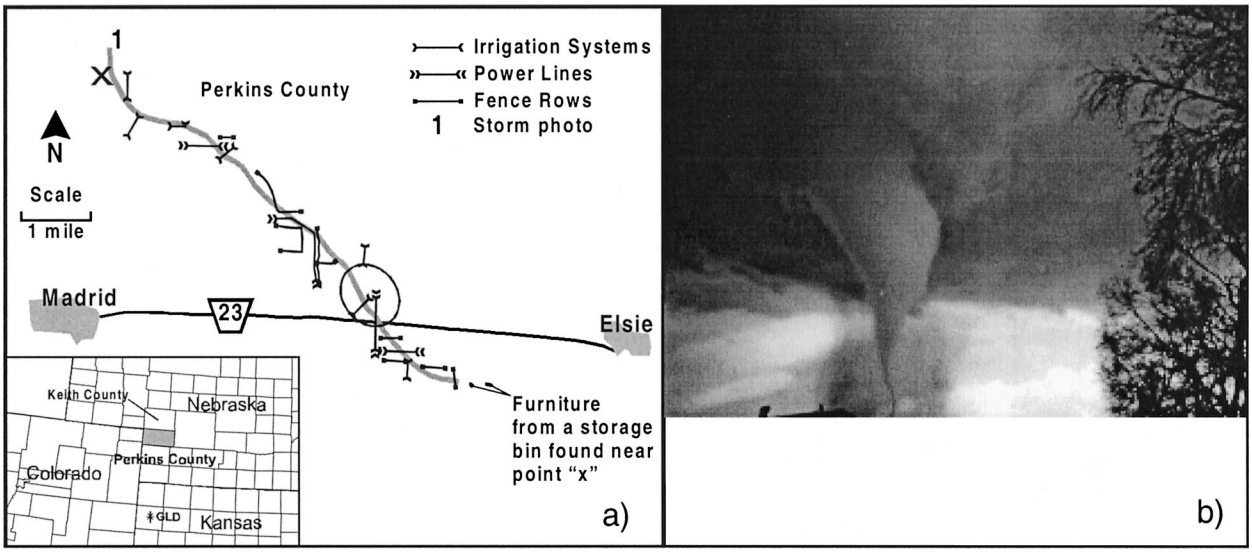

FIG. 1. (a) Damage track of tornado through a portion of Perkins County, NE. Legend indicates the damage incurred by the tornado. The X indicates the location of several large storage bins destroyed by the tornado. (b) Photograph of a developing tornado taken from location 1 in (a).

face Observing System (ASOS), the Aviation Weather Observing System (AWOS), and the Surface Aviation Observation (SAO) network. Spatial surface mesoanalysis was completed by augmenting the NWS observations with 54 stations from the High Plains Climate Center's (HPCC) Automated Weather Data Network, which records hourly temperature, relative humidity, and wind vector data.

Upper-air data were obtained from the NWS rawinsonde network, with soundings taken at 0000 and 1200 UTC. In addition, hourly wind profiles were obtained for 24 stations contained in the Wind Profiler Demonstration Network.

Visible (1-km resolution), infrared (4 km), and water vapor (8 km) imagery were obtained at 15-min intervals from the *Geostationary Operational Environmental Satellite-8 (GOES-8).* Weather Surveillance Radar-1988 Doppler (WSR-88D) level-II data from Goodland, Kansas (KGLD), were also processed and evaluated at 12-min temporal resolution.

Photographs and video of the tornado and parent supercell were obtained from several vantage points around the storm (Fig. 1). A detailed storm damage survey was conducted immediately after the event. This survey illustrated the main path of the tornado and significant damage as it traveled between Madrid and Elsie, Nebraska.

3. Analysis and storm evolution

a. Synoptic-scale environment

The synoptic-scale pattern at 1200 UTC 21 May 1995 featured a broad, low-amplitude ridge over the Rocky Mountain region with a trough extending from the Great Lakes through the central gulf coast area (Fig. 2). More important, the 850- and 700-hPa analyses revealed two short waves, one entering Montana from Alberta, and a second weaker one in west Texas (Figs. 2a and 2b). These two disturbances acted in concert to produce a significant area of low-level warm air advection over the high plains. Additionally, the short waves helped to transport moisture from west Texas northward to southwestern Nebraska where it played a critical role in destabilizing the local environment.

The 1200 UTC North Platte, Nebraska (LBF), sounding indicated that low-level winds were weak but veering from the surface to nearly 600 hPa (Fig. 3a). Both the 1200 and 0000 UTC soundings exhibited 0–6-km shear vectors of nearly 35 m s^{-1}, which are in the range found by Weisman and Klemp (1982, 1984, 1986) to be supportive of supercells, and greater than the average values found by Mead (1997) to be associated with tornadic supercells in the southern United States. Also, 0–3-km storm-relative helicity calculated from the 0000 UTC sounding was approximately 200 m^2 s^{-2}, which is slightly higher than the mean value (180 m^2 s^{-2}) found in a recent climatology of forecast parameters for significant tornado–producing supercells (Rassmussen and Blanchard 1998).

The 1200 UTC soundings from Dodge City (DDC) and Topeka (TOP) (not shown) showed an area of deep moisture over Kansas, with an 850-hPa moist axis extending through western Kansas into southern Nebraska. The approach and intensification of the lower-tropospheric short-wave trough to the north continued to back and intensify the low-level winds throughout the morn-

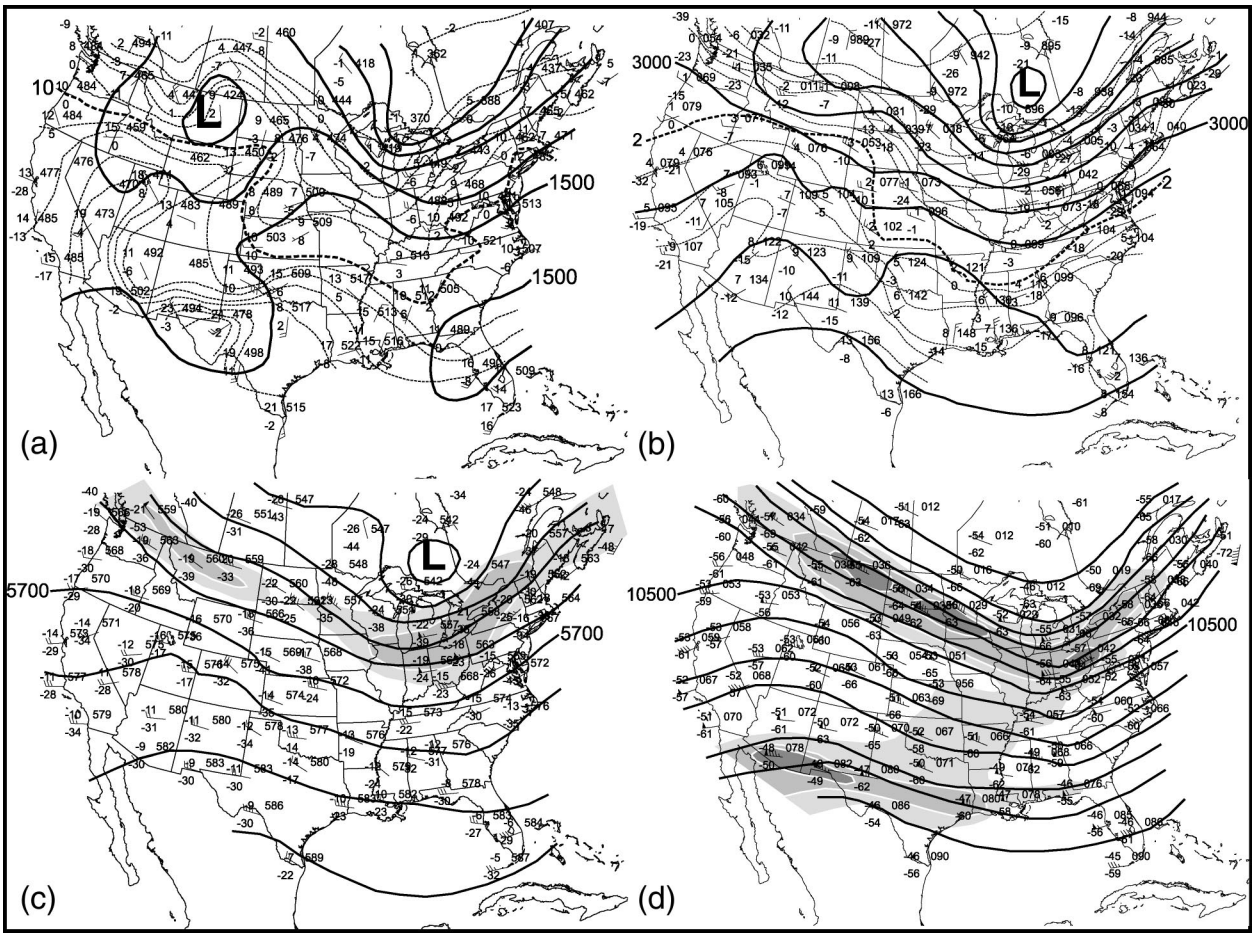

FIG. 2. (a) Subjective 850-hPa heights (gpm) and isotherms (°C) analyses for 1200 UTC 21 May 1995. The 1500-gpm isoheight and 10°C isotherm are references, and isolines are plotted at 30 gpm and 2°C, respectively. (b) Same as in (a) except for 700 hPa. The 3000-gpm isoheight and 2°C isotherm are referenced and isolines are plotted at 30 gpm and 2°C, respectively. (c) The 500-hPa heights (gpm) and isotachs (kt) at 1200 UTC 21 May 1995. The 5700-gpm isoheight is referenced, and isolines are plotted at 60-gpm intervals. The 50- and 60-kt isotachs are shaded. (d) Same as in (c) except for 250 hPa. The 10 500 gpm isoheight is referenced and contours are plotted at 60-gpm intervals. The 60-, 70-, and 80-kt isotachs are shaded. All station models are plotted using dewpoint temperature.

ing and early afternoon over the northern and central Great Plains. This transported moist, unstable air into the region from the southern Great Plains.

b. Mesoscale environment and storm evolution

The surface mesoscale environment during the morning featured an area of high pressure over north-central Kansas with a ridge extending through eastern Nebraska. Surface pressures were falling over eastern Wyoming and western Nebraska in response to the approaching short-wave trough to the north. Winds at the surface, west of the high, were southerly around 5 m s^{-1} and had begun to back in response to the approaching short wave. The visible satellite image from 1515 UTC (Fig. 4) shows an area of clouds and fog associated with the weak short-wave trough that moved through the area during the morning. Showers associated with this trough left behind a cool, moist, stable air mass over western Nebraska, northwestern Kansas, and northeastern Colorado, with temperatures at 1500 UTC in the low to mid-10s °C (50s °F) and dewpoints from 8° to 10°C. The area of clearing over western Nebraska and northern Colorado at 1515 UTC (Fig. 4) just west of the weak short-wave trough allowed for strong heating and resultant mixing in the convective boundary layer that led to the dissipation of fog and low clouds from west to east throughout the late morning and afternoon. In addition to rapid atmospheric destabilization due to solar heating within the clearing skies, the differential heating of the lower troposphere between the clear air to the west and cloudy, foggy air to the east allowed for the development of a north–south thermal gradient over extreme western Nebraska.

Early afternoon pressures continued to fall over the high plains, with a pressure trough–wind shift line lo-

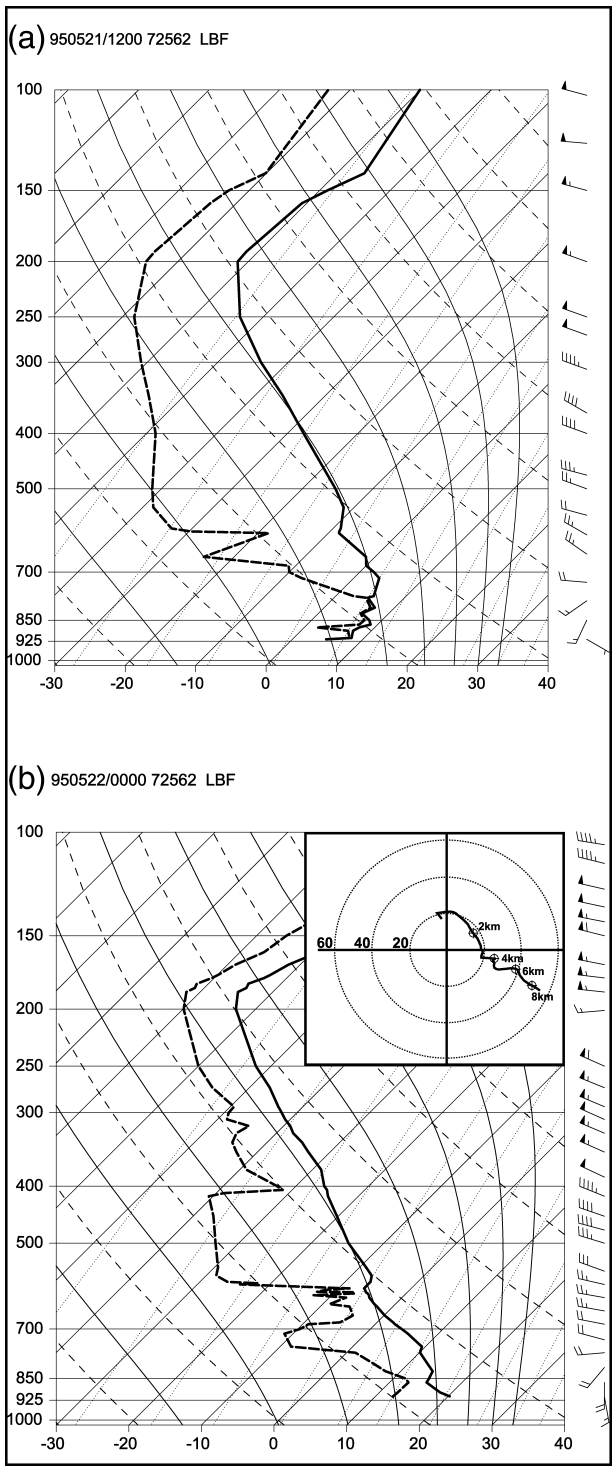

FIG. 3. (a) Skew T–log$p$ diagram for North Platte, NE, at 1200 UTC 21 May 1995. Temperatures are in degrees Celsius, and winds are in knots. (b) Same as in (a) but at 0000 UTC 21 May 1995 and including hodograph.

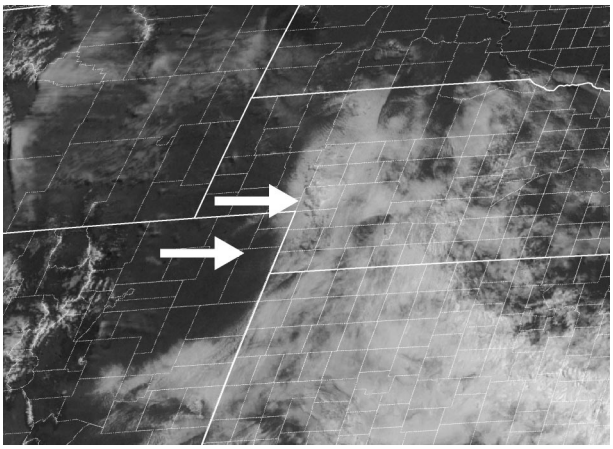

FIG. 4. *GOES-8* visible satellite image at 1515 UTC 21 May 1995. Arrows highlight the area of fog and rain and the clear region where destabilization took place.

cated through western Nebraska into northern Colorado. This feature was associated with a weak short-wave trough that moved through the area during the afternoon of 21 May. Strong mixing of the dry air under clear skies along with downsloping winds off the higher terrain west of the surface trough likely allowed for enhanced transport of higher westerly momentum to the surface. Ahead of the surface trough, winds continued to increase from the south, advecting moisture northward.

By 2000 UTC the atmosphere had become increasingly unstable under sunny skies in extreme southwest Nebraska as temperatures climbed into the low 20s °C (70s °F) and dewpoints had risen to near 16°C. A strong thermal gradient existed over southwest Nebraska at 1800 UTC, with temperatures in the low 20s °C (70s °F) in western Nebraska and northeastern Colorado and temperatures in the mid- to upper 10s °C (low 60s °F) throughout central Nebraska. The surface trough–wind shift line had moved slowly eastward and had begun to

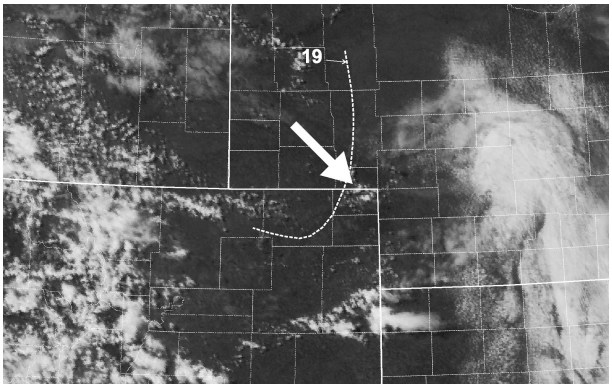

FIG. 5. *GOES-8* visible satellite image at 1945 UTC 21 May 1995. Dashed line indicates pressure trough–wind shift line analyzed at 1900 UTC. The arrow highlights the developing thunderstorm that eventually produced the tornado.

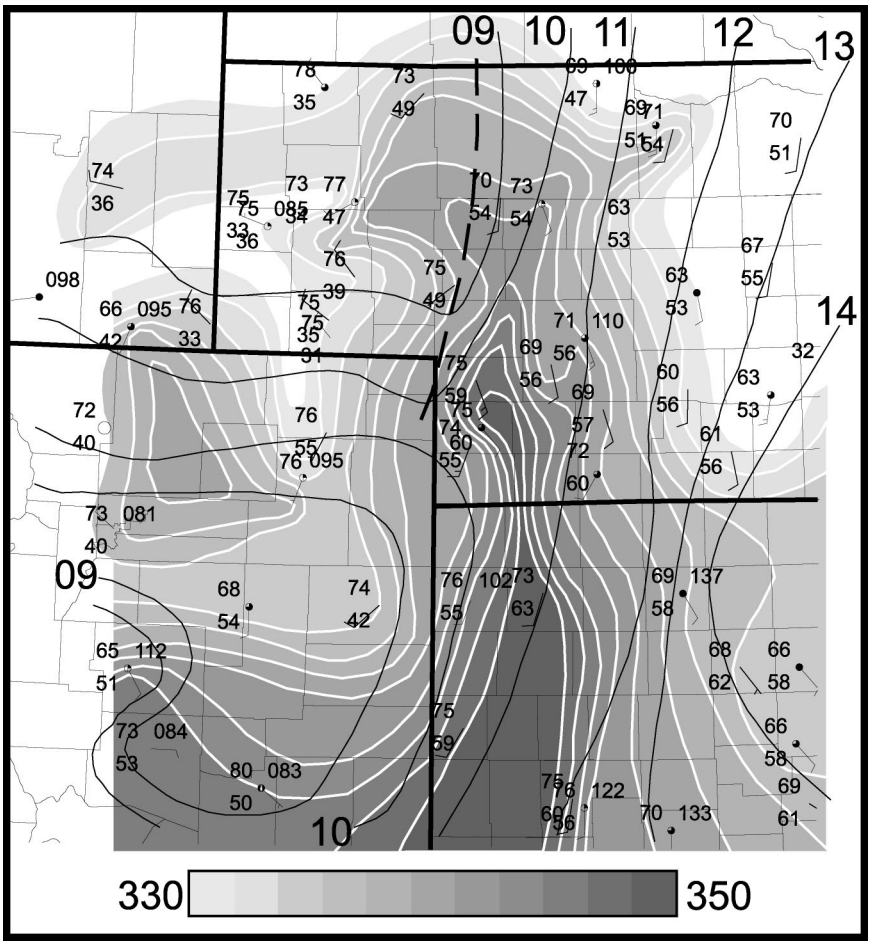

FIG. 6. Subjective surface isobar (hPa) and surface θ_e (K) analysis at 2200 UTC 21 May 1995. Isobars are plotted at 1-hPa intervals while surface θ_e is shaded at 2-K intervals. The dashed line denotes trough–wind shift axis.

bulge east-southeastward through northeastern Colorado and the Nebraska Panhandle. Winds to the east and southeast of the trough had increased and backed to the south-southeast by 2000 UTC with winds behind the trough primarily out of the west-northwest. Cumulus had developed along the leading edge of this convergent boundary, with a local enhancement of cumuliform development near the bulging apex (Fig. 5).

The small area of enhanced cumulus at the apex of the bulging trough began to rapidly intensify upon reaching the western edge of the θ_e ridge (approximately 2100 UTC). The resulting thunderstorm, which eventually became the tornadic supercell, continued to develop and move eastward through 2200 UTC.

At 2200 UTC, temperatures over extreme southwest Nebraska had climbed into the mid-20s °C (mid-70s °F) with dewpoints near 16°C (60°F) and southeast winds between 5 and 7.5 m s^{-1} (Fig. 6). The gradient of the θ_e axis over northern Kansas and southern Nebraska also intensified, with values approaching 344 K over extreme southwest Nebraska (Fig. 6). The surface trough–wind shift line continued to move eastward and by 2200 UTC intersected the western edge of the θ_e ridge. The position of the surface trough–wind shift line as interpolated from surface, satellite, and radar data from 1800 to 2300 UTC is illustrated in Fig. 7. The pressure trough–wind shift line moved eastward and southward through the afternoon while the θ_e gradient remained quasi-stationary over southwest Nebraska. At 2200 UTC, the HPCC station closest to the storm inflow had a temperature and dewpoint of 24° and 15°C (75° and 59°F), respectively. Modifying the 0000 UTC 22 May LBF sounding with this surface parcel yields large surface-based CAPE values approaching 3200 J kg^{-1} and a surface-based lifted index of −9, with little or no convective inhibition. This instability, combined with a favorable shear profile, produced a localized environment conducive to supercell formation (Fig. 3b).

c. Radar characteristics and storm-scale environment

The storm that would eventually produce the tornado in Perkins County developed around 2030 UTC near

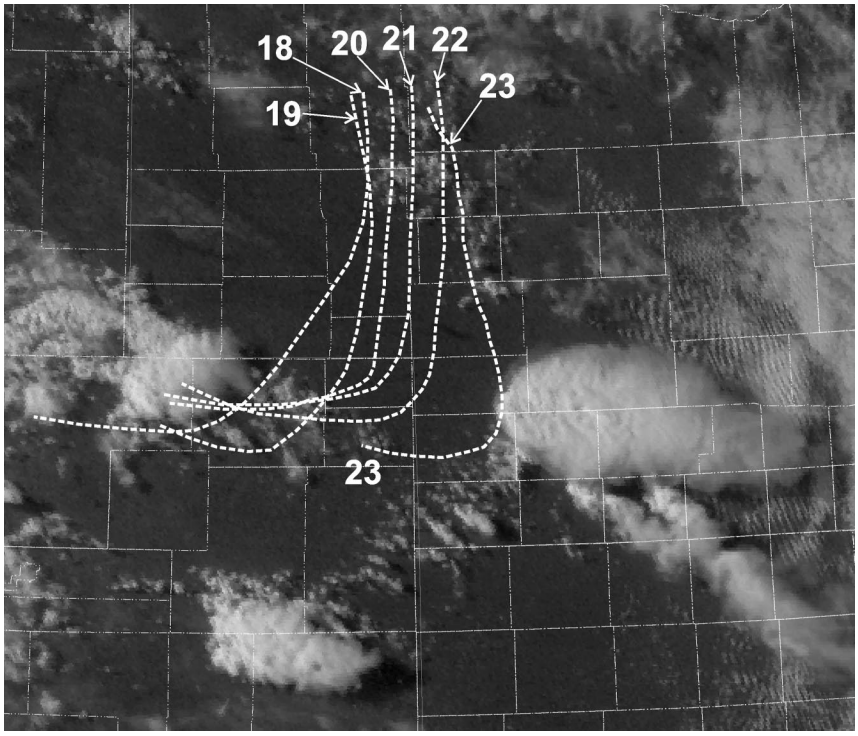

FIG. 7. Dashed line indicates the surface trough–wind shift line identified from satellite, radar, and surface analyses overlaid on the 2302 UTC 22 May 1995 *GOES-8* visible satellite image. Numbers represent time-relative locations.

the Keith–Perkins County line as a small, somewhat disorganized, area of weak (~20 dB*Z*) echoes as seen in the Goodland, Kansas (KGLD), WSR-88D base reflectivity and also noted in the visible satellite imagery (Fig. 5). From 2032 to 2056 UTC this area of convective activity began to evolve into one discrete cell while moving/developing east-northeastward just north of the Keith–Perkins County border and just ahead of the pressure trough–wind shift line. Additionally, another cell that had developed earlier was moving through Chase County and produced a distinct, northward-moving outflow boundary (Fig. 8).

Over the next hour, significant changes in storm structure ensued, culminating in tornadogenesis at 2233 UTC. Base reflectivities rapidly increased to over 70 dB*Z* by 2144 UTC (Figs. 8c and 8d). Simultaneously, the updraft strengthened and became more erect as a weak-echo region (WER) developed on radar (Fig. 9c; Lemon and Doswell 1979). By 2156 UTC, very little rotation was seen in the low and midlevels of the storm. At that time, an area of stronger inbound velocities began to develop on the west-northwest side of the updraft. At 2208 UTC a pronounced inflow notch and pendant echo developed and rotation became evident within the updraft. An area of stronger inbound velocities on the western side of the updraft were collocated with the leading edge of the pendant echo.

Additionally, the outflow boundary produced by convection to the south of the storm continued progressing northward as seen in radar and satellite imagery (Fig. 9). Relative positions of the outflow boundary identified and plotted from radar and satellite imagery through 2208 UTC indicated a northward velocity of approximately 8.7 m s^{-1} (Figs. 10a and 10b). The outflow boundary became less identifiable on radar after 2208 UTC primarily because the radar beam altitude at base elevation was 1.7 km over central Perkins County. However, assuming a constant northward progression, the outflow boundary would have collided with the supercell in Perkins County just prior to tornadogenesis (Figs. 10c and 10d).

4. Discussion

It appears the tornadic thunderstorm initiated in the very unstable air forced upward by localized convergence along the bulging pressure trough–wind shift line (Fig. 7). As the storm moved eastward, intensification ensued. This rapid intensification was likely the result of release of greater instability as the thunderstorm moved along and into the θ_e axis. The storm continued to intensify and develop into a supercell, moving slowly southeastward (Fig. 7). Using the supercell motion technique of Bunkers et al. (2000), the expected supercell motion given the shear evident in the 0000 UTC North Platte sounding is nearly identical to the observed mo-

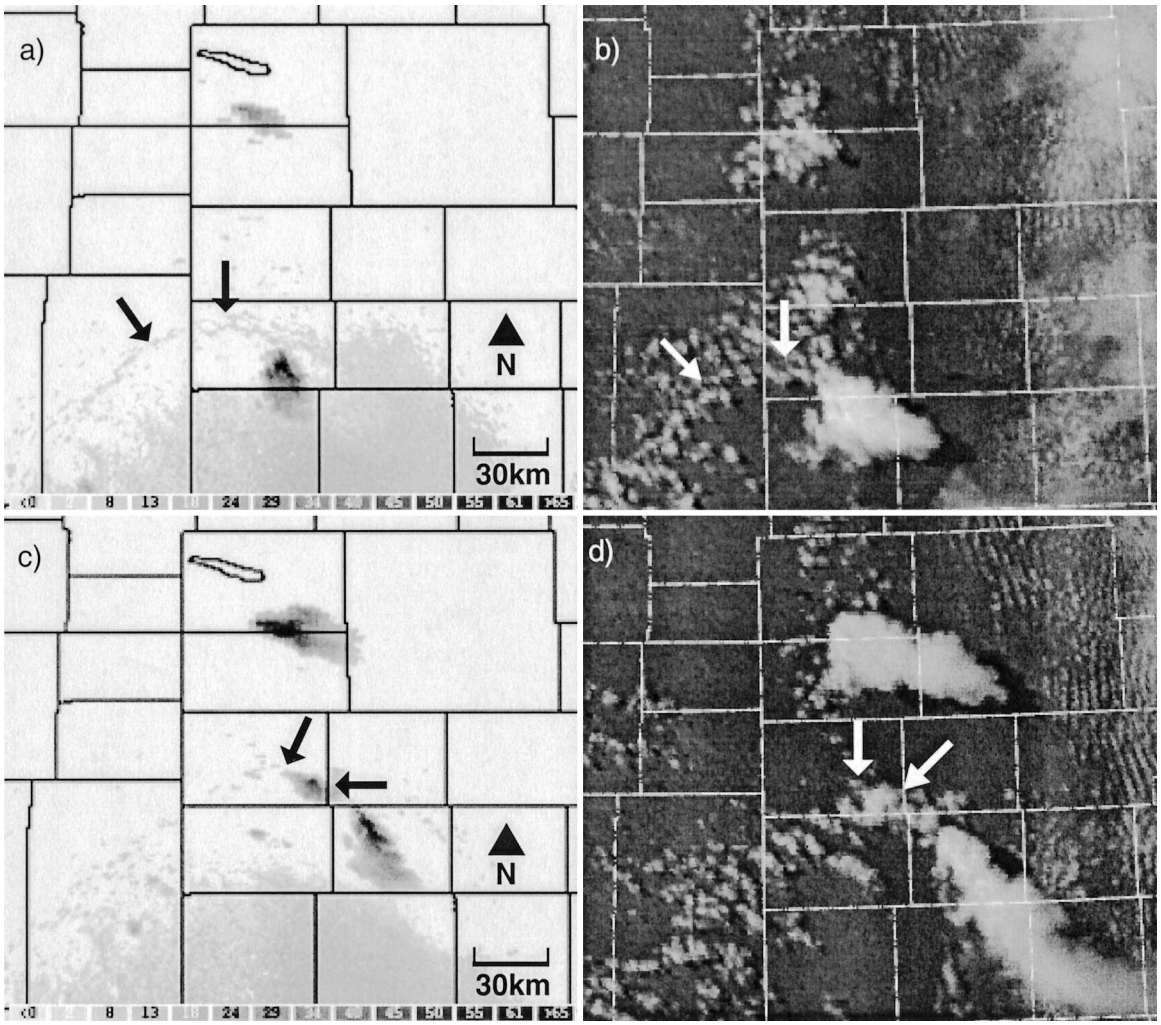

FIG. 8. (a) Grayscaled WSR-88D base reflectivity image at 2056 UTC 21 May 1995. (b) *GOES-8* visible satellite image at 2045 UTC 21 May 1995. (c) Same as in (a) but at 2144 UTC 21 May 1995. (d) Same as in (b) but at 2145 UTC 21 May 1995. Arrows indicate location of outflow boundary and enhanced convection due to this boundary.

tion of this storm. This deviant motion enhanced storm-relative inflow, helicity, and subsequent storm rotation. As the storm continued to move southeastward, it collided with a northward-moving outflow boundary. We speculate that this interaction of the storm with the outflow boundary over extreme southwest Nebraska was instrumental in enhancing storm rotation and tornado potential.

This investigation underlines the importance of recognizing relatively diffuse mesoscale features that can interact to create a local environment conducive to strong tornadogenesis. Although the synoptic environment was not favorable for a widespread tornado outbreak on 21 May 1995, multiscale interactions led to the development of a localized region favorable for mesocyclone and subsequent tornado development. Forecasters need to be cognizant of the interaction of mesoscale features that can lead to significant storm intensification or risk overlooking the development of a strong to violent tornado with relatively short spatial and temporal characteristics.

An ongoing aspect of this investigation involves estimating the wind speeds near the tornado by utilizing photogrammetry. Global positioning system (GPS) measurements along the tornado's path and the locations of the photographers and videographers have been sampled in order to estimate the speed of debris traveling around the cyclone. Results from this research will be disseminated at a later date.

Acknowledgments. The authors thank Bill Cooper, father of SC, and Walker Ashley at the Climatology Research Laboratory, The University of Georgia, for conducting the damage survey and processing the WSR-88D level-II data, respectively. The authors also thank Dr. John Scala, two anonymous reviewers, and Dr. Rob-

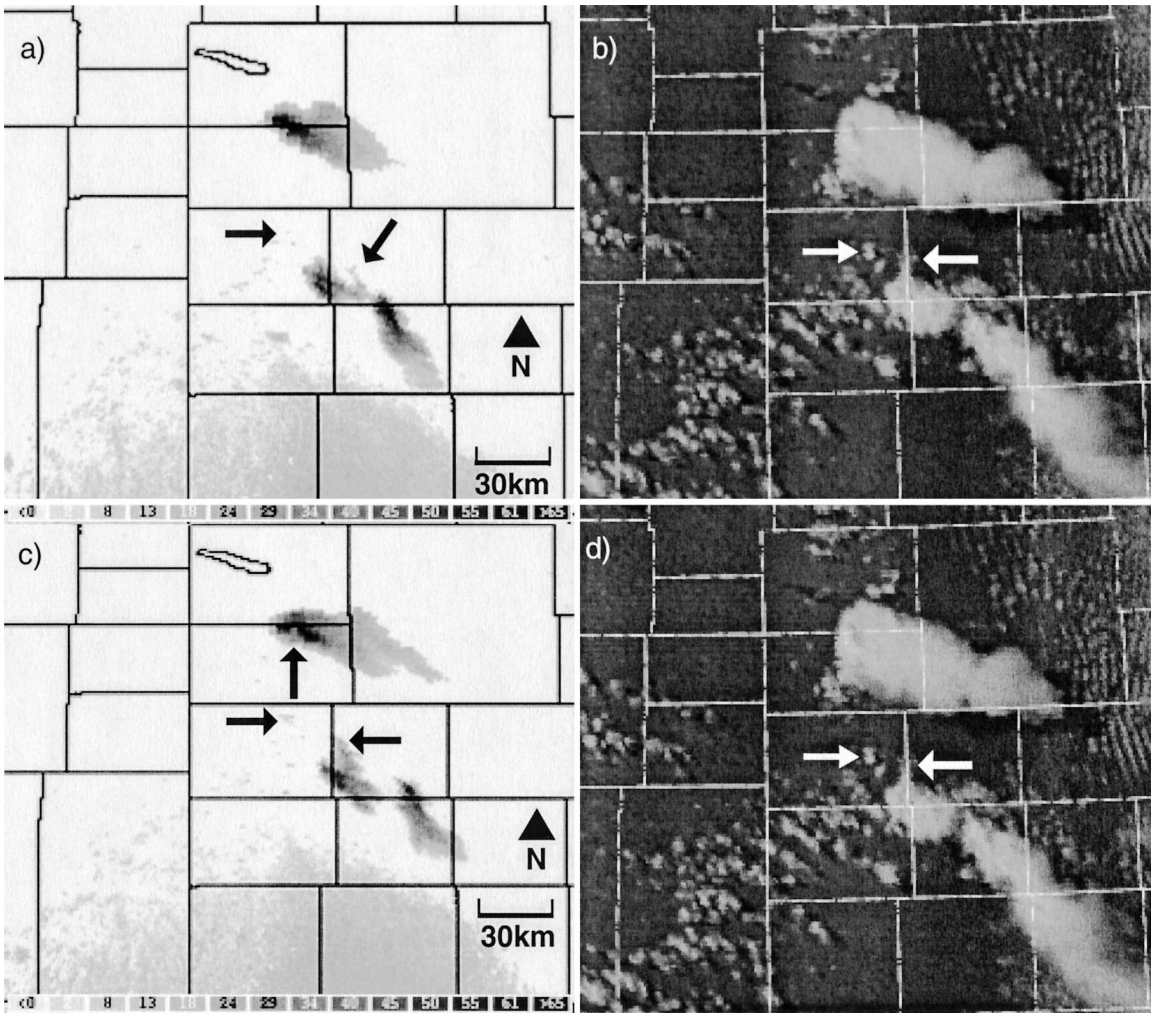

FIG. 9. (a) Grayscaled WSR-88D base reflectivity image at 2156 UTC 21 May 1995. (b) *GOES-8* visible satellite image at 2202 UTC 21 May 1995. (c) Same as in (a) but at 2208 UTC 21 May 1995. (d) Same as in (b). Arrows indicate weak echo notch and enhanced convection due to convergence along the northward-moving outflow boundary.

ert Maddox, editor, for their constructive comments, suggestions, and guidance during the review process. Many improvements were made to this manuscript by these individuals.

APPENDIX

Equivalent Potential Temperature Calculation

The equivalent potential temperature (θ_e) values for the High Plains Climate Center's stations were computed manually using interpolated sea level pressure obtained from a subjective analysis of the sea level pressure field from NWS first-order ASOS and AWOS stations. After assigning each high plains station a sea level pressure value, a standard atmospheric lapse rate and previous 12-h average ambient surface temperature were used along with station elevations to reduce sea level pressure to station pressure according to the following equation:

$$p_2 = p_1 \exp\{-g/[RT(Z_2 - Z_1)]\}$$

where p_1 is mean sea level pressure, p_2 is the station pressure, g is the acceleration due to gravity (9.80665 m s^{-2}), R is the gas constant for dry air (=287.04 J kg^{-1} K), T is the 12-h average ambient surface temperature in kelvins, and $(Z_2 - Z_1)$ is the station elevation in meters. This method is consistent with that used by the ASOS stations to convert between station and sea level pressure (Chu 1994). After computing station pressure, surface temperatures and dewpoints were used to calculate θ_e for each station. Sensitivity tests of calculated θ_e using 1-hPa variances in interpolated sea level pressure produced variances of approximately 0.1 K, or about one order of magnitude less than the implied accuracy of 1 K used in the analysis.

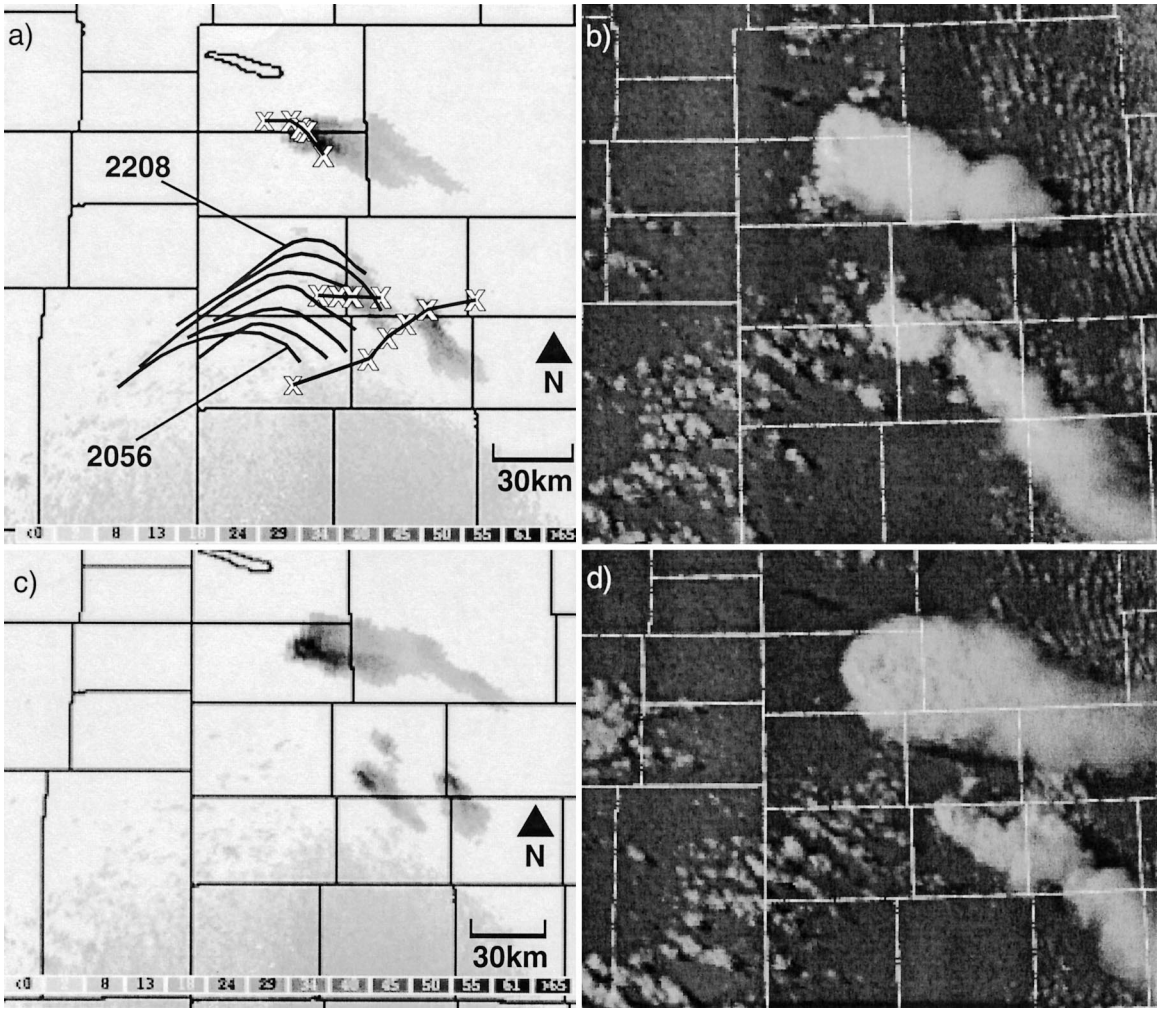

FIG. 10. (a) Grayscaled WSR-88D base reflectivity image at 2208 UTC 21 May 1995. Series of black lines indicates the progression of the outflow boundary as identified on radar. The Xs indicate individual cell motion through 2231 UTC. (b) *GOES-8* visible satellite image at 2202 UTC 21 May 1995. (c) Grayscaled WSR-88D base reflectivity image at 2231 UTC 21 May 1995. (d) Same as in (b) but at 2232 UTC 21 May 1995.

REFERENCES

Bunkers, M. J., B. A. Klimowski, J. W. Zeitler, R. L. Thompson, and M. L. Weisman, 2000: Predicting supercell motion using a new hodograph technique. *Wea. Forecasting,* **15,** 61–79.

Chu, R., 1994: Algorithms for the Automated Surface Observing System (ASOS). ISL Office Note 94-4, NWS/OSD, 106 pp.

Lemon, L. R., and C. A. Doswell III, 1979: Severe thunderstorm evolution and mesocyclone structure as related to tornadogenesis. *Mon. Wea. Rev.,* **107,** 1184–1197.

Maddox, R. A., L. R. Hoxit, and C. F. Chappell, 1980: A study of tornadic thunderstorms interactions with thermal boundaries. *Mon. Wea. Rev.,* **108,** 1866–1877.

Markowski, P. M., E. N. Rasmussen, and J. M. Straka, 1998: The occurrence of tornadoes in supercells interacting with boundaries during VORTEX-95. *Wea. Forecasting,* **13,** 852–859.

Mead, C. M., 1997: The discrimination between tornadic and nontornadic supercell environments: A forecasting challenge in the southern United States. *Wea. Forecasting,* **12,** 379–387.

Miller, R. C., 1972: Notes on the analysis and severe-storm forecasting procedures of the Air Force Global Weather Central. AWS Tech. Rep. 200 (rev.), Headquarters, Air Weather Service, Scott Air Force Base, IL, 190 pp.

NCDC, 1995: *Storm Data.* Vol. 37, No. 5, 131–132.

Purdom, J. F. W., 1976: Some uses of high-resolution GOES imagery in the mesoscale forecasting of convection and its behavior. *Mon. Wea. Rev.,* **104,** 1474–1483.

Rasmussen, E. N., and D. O. Blanchard, 1998: A baseline climatology of sounding-derived supercell and tornado forecast parameters. *Wea. Forecasting,* **13,** 1148–1164.

——, S. Richardson, J. M. Straka, P. M. Markowski, and D. O. Blanchard, 2000: The association of significant tornadoes with a baroclinic boundary on 2 June 1995. *Mon. Wea. Rev.,* **128,** 174–191.

Weisman, M. L., and J. B. Klemp, 1982: The dependence of numerically simulated convective storms on vertical wind shear and buoyancy. *Mon. Wea. Rev.,* **110,** 504–520.

——, and ——, 1984: The structure and classification of numerically simulated convective storms in directionally varying wind shears. *Mon. Wea. Rev.,* **112,** 2479–2498.

——, and ——, 1986: Characteristics of isolated convective storms. *Mesoscale Meteorology and Forecasting,* P. S. Ray, Ed., Amer. Meteor. Soc., 331–358.